Cluster variation theory of the paramagnetic anisotropy in MnF_2 susceptibilities

L. F. Libelo and R. L. Kligman
Naval Surface Weapons Center, White Oak, Silver Spring, Maryland 20910

Tomagasu Tanaka
Ohio University, Athens, Ohio 45701

(Received 5 August 1976; revised manuscript received 7 September 1977)

The cluster-variation theory is used to predict the anisotropy in the paramagnetic susceptibilities for the uniaxial antiferromagnet MnF_2. A Heisenberg model is assumed where the Hamiltonian includes dipole-dipole interaction, the source for the anisotropy. The sensitivity of the anisotropy to the number of dipole pairs permitted to interact is explicitly demonstrated. The effective g factor for the unpaired electrons in the Mn^{2+} ion is obtained from the anisotropy calculations.

I. INTRODUCTION

Manganese fluoride possesses a magnetic crystal structure that is relatively simple. Consequently this material has been well studied, experimentally and theoretically. Experimental studies have been quite extensive over the past 20 years. In particular, the temperature dependence of the anisotropic susceptibilities has been of interest to a number of investigators,[1-6] and serves as the basis for the present paper. The difference between the susceptibility measured along the easy direction and that found for the hard direction constitutes the anisotropy. Many theories have been proposed to explain the results obtained by Griffel and Stout.[2,3] In the latter data the anisotropy increases as the temperature is lowered. Near twice the Néel temperature, a maximum is reached. The anisotropy subsequently decreases becoming negative at a temperature approximately 10% higher than the Néel temperature. Griffel and Stout explain this behavior in terms of exchange forces which couple the spins together in groups, which produce a long-range order in the neighborhood of the critical temperature. Keffer[7] found that about 85% of the anisotropy was attributed to the long-range dipole-dipole interaction, the remainder being associated with the interaction of paramagnetic ions and their surrounding crystalline fields which produces a spin-orbit coupling. His calculations are based on classical dipole sums and the Weiss molecular field approximation along with the experimental value for the powder susceptibility as measured by Bizette and Tsai.[8] He was unable, however, to reproduce the measured maximum in the anisotropy. Instead, he found a monotonically increasing behavior with decreasing temperature down to T_N. Short-range exchange forces are cited as the mechanism for the maximum and subsequent negative anisotropy. Yosida,[9] using the Van Vleck model, found the anisotropy of the susceptibility at high temperature. He assumes the anisotropy originates from the action of the crystalline electric field on the Mn^{2+} ion combined with the spin-orbit interaction. A high-temperature power series in the partition function is generated, from which the anisotropy is determined. Its temperature behavior is monotonic and again no maximum is present. Nakamura[10] assumes that in some manner, the details of which are not known, the anisotropy energy of coupled spins increases as the Néel temperature is approached from above, in such a way that the energy becomes infinite at the critical temperature. Consequently, the anisotropy in the susceptibility is negative just above and has a square root singularity at the critical point. Treating the spins as classical vectors, and assuming the anisotropy is somehow crystalline field in origin, the anisotropy is expressed in terms of a spin-pair correlation function, where interactions between nearest-neighbor pairs are specifically taken into account. As a result of his approximations which force the required qualitative behavior on the temperature dependence of the anisotropy in the susceptibility, Nakamura's results are necessarily in fairly good agreement with Griffel and Stout's measurements. Heller[6] made nuclear magnetic resonance measurements and from this was able to deduce the sublattice magnetization in the neighborhood of the transition temperature. He also made measurements of quantities proportional to the parallel and perpendicular susceptibilities in the paramagnetic state. The temperature behavior of this data, in combination with the anisotropy data of Griffel and Stout below the Néel temperature shows the susceptibility in the anisotropy goes to zero just *below* and quite close to the Néel temperature. This is in direct conflict with the empirical results of Griffel and Stout showing that

this occurs above T_N. Heller's qualitative behavior of the paramagnetic susceptibility anisotropy is nevertheless in agreement with that of Griffel and Stout's, in that both reveal a maximum just above the transition temperature and then a monotonic decrease with increasing temperature. Although the temperature at which the anisotropy changes sign differs by only a few degrees, according to the different investigators, the uncertainty as to its occurrence above or below the Néel temperature is significant.

A number of theorists have recently made attempts to reproduce this behavior. Libelo and Tanaka[11] use the self-consistent–cluster-variation technique[12] to obtain the susceptibility anisotropy above the Néel temperature, assuming a pseudodipolar-anisotropy energy. The results are somewhat disappointing in that with decreasing temperature, monotonically increasing anisotropy is found. Itoh and Kanamori[13] used spin-wave theory to find the parallel and perpendicular susceptibilities below the Néel temperature. Their results are in good agreement with the data of Trapp and Stout up to temperatures as high as $\frac{2}{3}T_N$. This fails, however, to cover the temperature range of interest, namely the immediate neighborhood of the phase transition.

We shall use the self-consistent–cluster-variation method to calculate the paramagnetic susceptibilities. The anisotropy energy will be represented by the dipole-dipole interaction, consistent with the findings of many investigators. The theory will be restricted to the two-spin correlation limit. Nearest-neighbor dipole interactions are considered first, then next-neighbors and so on until many neighbor pairs are correlated to each other. The strength of the interaction will be determined from a comparison of the theoretical results to high-temperature data. The effective g factor of the unpaired elections in the Mn^{2+} ion will be found as well.

II. HEISENBERG SPIN HAMILTONIAN INCLUDING DIPOLE-DIPOLE INTERACTION

Single-crystal manganous fluoride possesses the tetragonal rutile crystal structure.[14,15] In the crystallographic unit cell the Mn^{2+} ions are located at the corners and the body center of the tetragonal cell. The c axis is taken along the foreshortened direction.

Six F^- ions, forming an irregular octahedron, surround each Mn^{2+} ion located at the center of the octahedron as can be seen in Fig. 1. Low-temperature neutron-diffraction studies[16,17] have determined the ordered magnetic structure of MnF_2. These neutron experiments reveal successive planes of Mn^{2+} ions aligned normal to the c axis. The spins in these planes of Mn^{2+} ions, alternate from parallel to the c axis in one plane to antiparallel to the c axis in the next plane and continue in this manner along the c axis. For this reason we can conveniently consider the Mn^{2+} ions to be distributed over two magnetic sublattices.

The dipole-dipole interaction is represented by the term

$$K\vec{S}_j \cdot (\vec{e}_{jk}\vec{e}_{jk} - \bar{I}/3) \cdot \vec{S}_k r^{-3}, \tag{2.1}$$

where K is a measure of the interaction strength for a dipole-dipole pair. The quantity $\vec{e}_{jk}$ is the unit vector between the jth and kth lattice points, $\bar{I}$ is the unity dyad, and r is the distance between these lattice points. In accord with Keffer's considerations,[7] we shall ignore the much smaller crystalline-field anisotropy. Then the spin Hamiltonian for the magnetic system of ions may be expressed as

$$\begin{aligned}
\mathcal{H} = {} & H_z\left(\sum_\alpha S_{\alpha z} + \sum_\beta S_{\beta z}\right) + H_x\left(\sum_\alpha S_{\alpha x} + \sum_\beta S_{\beta x}\right) + 2J_1\left(\sum_{\langle j(\alpha),\, k(\alpha)\rangle} \vec{S}_{j(\alpha)} \cdot \vec{S}_{k(\alpha)} + \sum_{\langle j(\beta),\, k(\beta)\rangle} \vec{S}_{j(\beta)} \cdot \vec{S}_{k(\beta)}\right) \\
& + 2J_2 \sum_{\langle \alpha,\beta\rangle} \vec{S}_\alpha \cdot \vec{S}_\beta + 2J_3\left(\sum_{\langle j(\alpha),k(\alpha)\rangle} \vec{S}_{j(\alpha)} \cdot \vec{S}_{k(\alpha)} + \sum_{\langle j(\beta),\, k(\beta)\rangle} \vec{S}_{j(\beta)} \cdot \vec{S}_{k(\beta)}\right) \\
& + \sum_n K_n \sum_{\langle j(\alpha),\, k(\alpha)\rangle_n} \vec{S}_{j(\alpha)}\left(\vec{e}_{jk}\vec{e}_{jk} - \frac{\bar{I}}{3}\right) \cdot S_{k(\alpha)} r_n^{-3} + \sum_n K_n \sum_{\langle j(\beta),\, k(\beta)\rangle_n} \vec{S}_{j(\beta)}\left(\vec{e}_{jk}\vec{e}_{jk} - \frac{\bar{I}}{3}\right) \cdot \vec{S}_{k(\beta)} r_n^{-3} \\
& + \sum_{n'} K_{n'} \sum_{\langle \alpha,\, \beta\rangle_{n'}} \vec{S}_\alpha\left(\vec{e}_{\alpha\beta}\vec{e}_{\alpha\beta} - \frac{\bar{I}}{3}\right) \cdot \vec{S}_\beta r_{n'}^{-3}.
\end{aligned} \tag{2.2}$$

Clearly the notation in this Hamiltonian requires some elaboration. The two magnetic sublattices are labeled by α and β. The first sum is the Zeeman energy in the external magnetic field H_z and the second sum is that in the external field H_x. Then following these are the first-neighbor intrasublattice-exchange energies, the second-neighbor antiferromagnetic-intersublattice-exchange energy, and the third-neighbor intrasublattice-exchange energies. Lastly we have the dipole-dipole

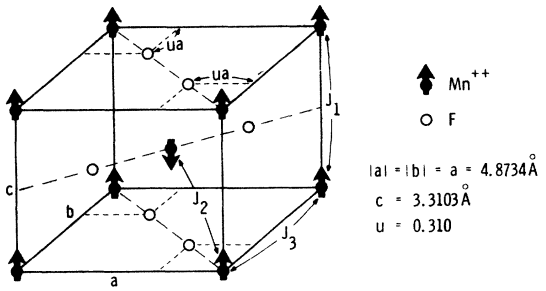

FIG. 1. MnF_2 crystallographic unit cell. The first subshell of dipoles coincides with those comprising the unit cell. Nearest neighbors lie along the c axis and second neighbors along the body diagonal.

interaction energies. The indices n and n', respectively, denote whether the neighbor pair participating in the interaction resides either on the same sublattice or on different sublattices. For example, $n=1$ denotes the nearest-neighbor pair where in fact both members of the pair reside on the same sublattice. Again, only as a matter of convenience, we shall define the dipole subshell. Using any dipole as our reference, a dipole subshell consists of all those dipole neighbors that are oriented parallel to the reference. The termination of the subshell is determined by the neighbor that is oriented antiparallel to the reference and is included in the subshell as well. In MnF_2, the nearest-neighbor dipole is oriented parallel to the reference, which for convenience may be taken at a corner of the unit cell. The second-nearest neighbor is oriented antiparallel to the reference. Thus, the first and second neighbors comprise the first subshell. This is clear from Fig. 1. In the same manner we may obtain successive dipole shells. This techniques is a rather liberal extension of that introduced by Evjen[18] and applied to ionic crystal lattices. For convenience of bookkeeping we have adapted it to the magnetic sublattices in our problem. The primed position vectors denote the direction in the XY plane perpendicular to the applied field H_x.

Antiferromagnetic spin wave dispersion in MnF_2 was measured by means of inelastic neutron scattering.[19] Using spin-wave theory, values for the exchange integrals were obtained. J_1, J_2, and J_3 are the first, second and third-neighbor exchange integrals along the c axis, the body diagonal axis, and the a-b axes, respectively. The obtained values are

$$J_1 = 0.32\ ^\circ\mathrm{K}, \quad J_2 = -1.76\ ^\circ\mathrm{K}, \quad J_3 < 0.05\ ^\circ\mathrm{K} \approx 0.$$

The second-neighbor exchange J_2 is in close agreement to that found by Trapp and Stout[5] who combined their measurements of the low-temperature perpendicular susceptibility with the antiferromagnetic-resonance-frequency measurements of Nethercot and Johnson.[20] They found $J_2 = -1.76\ ^\circ$K and for the nearest-neighbor exchange an antiferromagnetic value $J_1 = -1.3\ ^\circ$K. Brown *et al.*[21] made paramagnetic resonance measurements on dilute solid solutions of MnF_2 mixed with ZnF_2 and found for the nearest-neighbor exchange $J_1 = 0.2 \pm 0.1\ ^\circ$K and for the second-neighbor exchange $|J_2| \approx 2\ ^\circ$K. The discrepancy in the nearest-neighbor exchange integral is not understood. In this paper an attempt is made to resolve the sign of the exchange by performing calculations with the values found by Low *et al.*,[19] for J_1 equal to both $=0.32\ ^\circ$K and $-0.32\ ^\circ$K.

III. CLUSTER-VARIATION METHOD AND REDUCED EFFECTIVE-DENSITY MATRICES

In earlier papers[12,22] the cluster-variation method was presented in considerable detail. We shall therefore omit detailed development of the theory here. In the treatment of MnF_2 we shall ignore all contributions to the entropy beyond that due to two-spin correlation. Thus we may write the entropy[12] as

$$\begin{aligned} -k_0^{-1}S = &\sum_j \mathrm{tr}_j \rho^{(1)}(j) \ln \rho^{(1)}(j) \\ &+ \sum_{j>k} [\mathrm{tr}_{jk} \rho^{(2)}(j,k) \ln \rho^{(2)}(j,k) \\ &- \mathrm{tr}_j \rho^{(1)}(j) \ln \rho^{(1)}(j) \\ &- \mathrm{tr}_k \rho^{(1)}(k) \ln \rho^{(1)}(k)]. \end{aligned} \tag{3.1}$$

The density matrices in Eq. (3.1) satisfy the explicit reducibility conditions

$$\mathrm{tr}_j \rho^{(1)}(j) - 1 = 0, \tag{3.2}$$

$$\mathrm{tr}_k \rho^{(2)}(j,k) - \rho^{(1)}(j) = 0. \tag{3.3}$$

An approximately equivalent set of reducibility conditions may be used.[22] They are

$$\mathrm{tr}_j S_{jz} [\mathrm{tr}_k \rho^{(2)}(j,k) - \rho^{(1)}(j)] = 0, \tag{3.4}$$

$$\mathrm{tr}_{jk} \rho^{(2)}(j,k) = 1. \tag{3.5}$$

Equation (3.4) is a consistency condition on the first moment of magnetization, i.e., we are only requiring that the first moment be the same whether $\rho^{(1)}$ or $\rho^{(2)}$ is used to calculate it. In the presence of external x and z component fields, variations of the free energy with respect to $\rho^{(1)}(j)$ and $\rho^{(2)}(j,k)$ readily yield the required one- and two-spin reduced-density matrices. The reduced-density matrices contain the Lagrange undetermined parameters $\lambda_{l\alpha}$, $\lambda_{l\beta}$, and $\lambda_{\beta\alpha}$ ($\mu_{l\alpha}$, $\mu_{l\beta}$, and $\mu_{\alpha\beta}$) which are readily interpreted physically as $z(x)$ components of the local fields. For ex-

ample, $\lambda_{l\alpha}$ is the z component of local field at a dipole located at an α site. The source of this field is a dipole on the same sublattice positioned at $\vec{r}_l$. These local fields may be determined approximately from the consistency conditions for the first moment of the magnetization. The expectation value of the magnetization must be the same whether one averages using a one- spin or two-spin density matrix.

IV. THE PARAMAGNETIC SUSCEPTIBILITIES

Above the Néel temperature, in the paramagnetic phase, the local fields may be expanded in a power series in a small externally applied field. This results in a separation of the local fields into spontaneous and induced parts, thus

$$\lambda_{ij} = \lambda_{ij}^{(0)}(T) + H_z\lambda'_{ij}(T) + \cdots ,$$

$$\mu_{ij} = H_x\mu'_{ij}(T) + \cdots .$$

Of course above the Néel temperature the spontaneous local fields $\lambda_{ij}^{(0)}$ vanish for all temperatures. For a very small external field, the induced portion of the local field is approximately linearly dependent on the external field. We can then write

$$\lambda_{jk}(H_z, T) \approx H_z\lambda'_{jk}(T), \tag{4.1a}$$

$$\mu_{jk}(H_x, T) \approx H_x\mu'_{jk}(T), \tag{4.1b}$$

for the z and x components of the induced local fields. Furthermore, above T_N the two magnetic sublattices are indistinguishable and we have

$$\begin{aligned} \lambda_{j(\alpha)k(\alpha)} &= \lambda_{j(\beta)k(\beta)} = \lambda_{k(\beta)j(\beta)}, \\ \lambda_{j(\alpha)k(\beta)} &= \lambda_{j(\beta)k(\alpha)} = \lambda_{k(\alpha)j(\beta)}. \end{aligned} \tag{4.2}$$

With the aid of these relations, we can eliminate the local-field parameters from the magnetization expressions. In this manner the longitudinal paramagnetic susceptibility, or the paramagnetic susceptibility parallel to the c axis, is found to be

$$\chi_{\parallel}(\theta) = \frac{\theta}{3}\left[\sum_n \frac{Z_n}{\phi_n(J_n, \theta)} + \sum_{n'} \frac{Z_{n'}}{\phi_{n'}(J_{n'}, \theta)} - [S(S+1)]^{-1}\left(\sum_n Z_n + \sum_{n'} Z_{n'} - 1\right)\right]^{-1}, \tag{4.3}$$

where, for example, we have introduced the function

$$\begin{aligned} \phi_n(J_n, \theta) = \frac{3}{2}\Bigg(&\sum_{\mathcal{S}=0}^{2S} \sum_{M=-\mathcal{S}}^{\mathcal{S}} M^2(1 + \theta K_n\gamma_n^{-3}\langle \mathcal{S}M|\vec{\mathcal{S}}_{j(\alpha)} \cdot \vec{e}_{jk}\vec{e}_{jk} \cdot \vec{\mathcal{S}}_{k(\alpha)}|\mathcal{S}M\rangle) \\ &\times \exp[\theta L_n\mathcal{S}(\mathcal{S}+1)] \Big/ \sum_{\mathcal{S}=0}^{2S} \sum_{M=-\mathcal{S}}^{\mathcal{S}} (1 + \theta K_n\gamma_n^{-3}\langle \mathcal{S}M|\vec{\mathcal{S}}_{j(\alpha)} \cdot \vec{e}_{jk}\vec{e}_{jk} \cdot \vec{\mathcal{S}}_{k(\alpha)}|\mathcal{S}M\rangle) \\ &\times \exp[\theta L_n\mathcal{S}(\mathcal{S}+1)]\Bigg) \quad \text{for } n = 1, 3, 4, 6, 7, 8, \ldots . \end{aligned} \tag{4.4}$$

$\phi_{n'}(J_{n'}, \theta)$ is a similar function for an intersublattice pair. In these equations the abbreviated quantity L_n appears which is defined by

$$L_m = 2J_m - K_m(3\gamma_m^3)^{-1} \quad \text{for } m = n \text{ or } n' . \tag{4.5}$$

It is merely the effective coefficient of $\vec{\mathcal{S}}_j \cdot \vec{\mathcal{S}}_k$. The quantities $\phi_n(J_n, \theta)$ and $\phi_n(J_{n'}, \theta)$ are derived from a perturbation expansion which was discussed in an earlier report.[22] Similarly, for the transverse paramagnetic susceptibility, i.e., perpendicular to the c axis, we obtain

$$\begin{aligned} \chi_{\perp}(\theta) = \frac{\theta}{3}\Bigg[&\sum_n \left(\frac{Z_n}{\psi_n(J_n, \theta)} + \frac{Z'_n}{\psi'_n(J_n, \theta)}\right) + \sum_{n'} \left(\frac{Z_{n'}}{\psi_{n'}(J_{n'}, \theta)} + \frac{Z'_{n'}}{\psi'_{n'}(J_{n'}, \theta)}\right) \\ &- [S(S+1)]^{-1}\left(\sum_n (Z_n + Z'_n) + \sum_{n'} (Z_{n'} + Z'_{n'}) - 1\right)\Bigg]^{-1}, \end{aligned} \tag{4.6}$$

where now we have introduced the functions $\psi_n(J_n, \theta)$, $\psi'_n(J_n, \theta)$, $\psi_{n'}(J_{n'}, \theta)$, and $\psi'_{n'}(J_{n'}, \theta)$. These four functions correspond to the two in Eq. (4.3). The additional relations arise from the difference between the X and Y directions. The anisotropy in the susceptibility is given by the difference between Eqs. (4.3) and (4.6). The quantities K_n and $K_{n'}$ are now determined by comparing at $T = 295.6$ °K the experimental high-temperature anisotropy data of Griffel and Stout with our results. These are fitted into agreement with the data by choosing the proper values for the dipole-dipole constants.

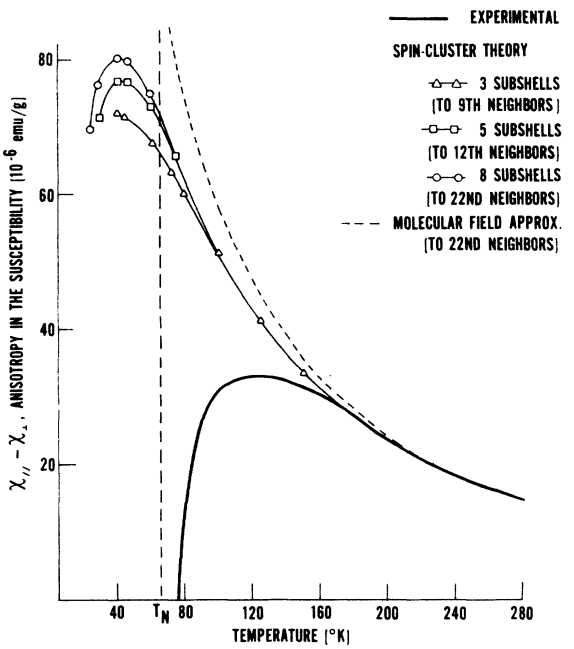

FIG. 2. Anisotropy in the susceptibility.

Figure 2 displays the calculated and measured temperature dependences of the anisotropy in the high-temperature region. The measured anisotropy shown is that of Griffel and Stout.[3] We show in Fig. 2 a family of curves for the anisotropy generated by successively increasing the number of interacting dipoles included in the calculation. For example, the curve labeled "3 subshells" incorporates the effect of 60 dipoles in the first three subshells, interacting pairwise. The corresponding dipole-dipole range of interaction extends to and includes the ninth nearest neighbor. As the number of interacting dipoles increases the anisotropy appears to increase only slightly for temperatures above but in the neighborhood of the phase-transition temperature. It is interesting to note that if one just formally extends the paramagnetic calculation down into the ordered phase a maximum does seem to appear in the anisotropy in the susceptibility. Nevertheless, it should be kept in mind that below T_N the spontaneous local-field contributions must be taken into account in order to obtain the proper temperature dependence of $\chi_{\parallel}$ and $\chi_{\perp}$ up to T_N. In the paramagnetic regime we find that the anisotropy in the susceptibility remains positive and increases as the temperature is decreased.

V. CONCLUSIONS

The cluster-variation theory in the two-spin correlation approximation predicts rather precisely the temperature dependence of the anisotropy in the susceptibility at temperature $T \gtrsim 160\,^{\circ}\mathrm{K}$. As shown in Fig. 2, if we require consistency for only the first moment of the magnetization, we obtain considerably better agreement with experiment then one obtains from Weiss molecular-field theory for all temperatures $T \geq T_N$. Recalling that $\chi_{\parallel} - \chi_{\perp}$ is several orders of magnitude smaller than either $\chi_{\parallel}$ or $\chi_{\perp}$ in the paramagnetic neighborhood of T_N, we conclude that the cluster-variation theory is consistent with Heller's finding[6] that the anisotropy goes negative below T_N. It would appear that the Griffel and Stout[3] results (Fig. 2) indicating that this sign change occurs at a point significantly higher than T_N requires more extensive measurement of the rather small anisotropy in the neighborhood of the phase-transition temperature. Only in this manner can the question concerning this prominent feature of the Griffel and Stout data be resolved once and for all. We again emphasize that Heller[6] found the anisotropy changing sign below but very nearly at T_N. He also found a maximum above T_N but quite close to it. This second prominent feature agrees only qualitatively with the earlier Griffel and Stout data. The latter (Fig. 2) found the maximum lying far out in the vicinity of $T \approx 2T_N$. It would again seem that more extensive measurement is called for to resolve this substantial discrepancy.

Unfortunately Weiss field theory leaves little room for improving its predicted values for MnF_2. However the cluster-variation method can still be made more accurate. Merely by requiring consistency of the second moment of the magnetization in the two-spin approximation we can obtain improved temperature dependence of anisotropy for $T \gtrsim T_N$. Hunter, Libelo, and Tanaka[23] have shown that including the requirement of consistency of the second moment does not affect T_N but does re-

TABLE I. Effective paramagnetic MnF_2 g factor. Variation of this parameter with sign of the small nearest-neighbor exchange interaction and with range of the dipole-dipole interaction is shown.

Total number subshells	g factor $J_1 > 0$	g factor $J_1 < 0$	Neighbor included in the subshells	Total no. coupling dipoles	Dipoles in outermost subshell
1	3.86	3.86	1 → 2	10	10
2	2.86	2.90	1 → 5	30	20
3	2.71	2.73	1 → 9	60	30
5	2.31	2.34	1 → 12	92	16
6	2.09	2.12	1 → 17	122	30
7	2.03	2.07	1 → 20	154	32
8	2.02	2.05	1 → 22	178	24

sult in small changes in the magnetization. Such an extension of the theory very likely may be crucial for resolving analytically the location of the maximum in the rather small anisotropy. This study is to be made and the results shall be reported on later. In summary then we note that the earlier measurements of the paramagnetic anisotropy in the MnF_2 susceptibility are not consistent with more recent independent measurements. Present theory yields results in closer agreement with the newer data but still requires further improvement.

Finally we show in Table I the effective g factor for MnF_2 as a function of the explicit range of dipole-dipole interaction taken into account as well as the effect of the sign of the small first-neighbor exchange interaction. It is clear in the Table that the g factor has pretty much converged to its effective value after 7 or 8 subshells are included. This is true for both $J_1 > 0$ and $J_1 < 0$.

[1]S. Foner, J. Phys. Radium 20, 336 (1949).
[2]M. Griffel and J. W. Stout, Phys. Rev. 76, 144 (1949).
[3]M. Griffel and J. W. Stout, J. Chem. Phys. 18, 1455 (1950).
[4]L. Corliss, Y. Delabarre, and N. Elliott, J. Chem. Phys. 18, 1256 (1950).
[5]C. Trapp and J. W. Stout, Phys. Rev. Lett. 10, 157 (1963).
[6]P. Heller, Phys. Rev. 146, 403 (1966).
[7]F. Keffer, Phys. Rev. 87, 608 (1952).
[8]H. Bizette and B. Tsai, C. R. Acad. Sci (Paris) 209, 205 (1939).
[9]K. Yosida, Prog. Theor. Phys. 6, 691 (1951).
[10]T. Nakamura, Phys. Rev. 128, 2500 (1962).
[11]L. F. Libelo and T. Tanaka, J. Appl. Phys. 39, 430 (1968).
[12]T. Morita and T. Tanaka, Phys. Rev. 145, 288 (1966).
[13]Y. Itoh and J. Kanamori, J. Phys. Soc. Jpn. 33, 315 (1972).
[14]P. P. Ewald and C. H. Hermann, Strukturbereicht (Leipz.) 1, 192 (1931).
[15]M. Griffel and J. W. Stout, J. Am. Chem. Soc. 72, 4351 (1950).
[16]R. A. Erickson and C. G. Shull, Phys. Rev. 83, 208 (1951).
[17]R. A. Erickson, Phys. Rev. 90, 779 (1953).
[18]H. H. Evjen, Phys. Rev. 39, 675 (1932).
[19]G. G. Low, A. Okazaki, R. W. H. Stevenson, and K. C. Turberfield, J. Appl. Phys. 35, 998 (1964).
[20]F. M. Nethercot and A. H. Johnson, Phys. Rev. 114, 705 (1959).
[21]M. R. Brown, B. A. Coles, J. Owen, and R. W. H. Stevenson, Phys. Rev. Lett. 7, 246 (1961).
[22]L. F. Libelo, R. L. Kligman, and T. Tanaka, Phys. Rev. 171, 531 (1968).
[23]P. Hunter, L. F. Libelo, and T. Tanaka, Bull. Am. Phys. Soc. 22, 376 (1977).